# Scanning and Mapping Strategies for CMB Experiments

E. L. Wright

## ABSTRACT

CMB anisotropy experiments seeking to make maps with more pixels than the 6144 pixels used by the *COBE* DMR need to address the practical issues of the computer time and storage required to make maps. A simple, repetitive scan pattern reduces these requirements but leaves the experiment vulnerable to systematic errors and striping in the maps. In this paper I give a time-ordered method for map-making with one-horned experiments that has reasonable memory and CPU needs but can handle complex *COBE*-like scans paths and $1/f$ noise.

## 1. Introduction

Many new CMB missions such as *COBRAS/SAMBA* have adopted scan patterns with a relatively small number of scan circles in order to simplify the data analysis. The very successful *COBE* pattern of cycloidal scans that cross through each pixel in many different directions is not used, and this leads to an increased sensitivity to systematic errors. These new missions have adopted a total power or one-horned approach to maximize sensitivity relative to the differential approach used by *COBE*. But this often leads to excess low frequency or $1/f$ noise.

## 2. Direct Imaging

A simple scan pattern with great circle scans perpendicular to the Sun line can lead to *striping* even in the absence of $1/f$ noise. The simplest reference pattern is to reference each pixel in the scan to the NEP. Thus the equation to be solved in the map-making for pixel $j$ which is the $i^{th}$ pixel in the $k^{th}$ scan is

$$T_j - T_{\text{NEP}} = S(i,k) - S(\text{NEP},k). \tag{1}$$

We assume that the samples $S(i,k)$ are uncorrelated (white noise) except for a constant baseline that has to be determined for each scan. But the baseline cancels out in this equation. The noise associated with this equation is $\sqrt{2}$ times the noise per pixel because two values are subtracted.

These observations can be inverted directly giving

$$
\begin{aligned}
T_{\text{NEP}} &= 0 \\
T_j &= S(i,k) - S(\text{NEP},k) \\
T_{\text{SEP}} &= \frac{2}{N} \sum_k [S(\text{SEP},k) - S(\text{NEP},k)]
\end{aligned}
\tag{2}
$$

$$\tag{3}$$

where the first line is an assumption for $T_{\rm NEP}$. This appears to be the approach described in the text of Janssen *et al.* (1996).

The covariance matrix can also be computed directly:

$$
\begin{aligned}
\langle T_{\rm SEP} T_{\rm SEP} \rangle &= \frac{4\sigma_1^2}{N} \\
\langle T_i T_{\rm SEP} \rangle &= \frac{2\sigma_1^2}{N} \\
\langle T_i T_i \rangle &= 2\sigma_1^2 \\
\langle T_i T_j \rangle &= \begin{cases} \sigma_1^2, & \text{if on the same scan;} \\ 0, & \text{otherwise.} \end{cases}
\end{aligned}
\tag{4}
$$

$$\tag{5}$$

The non-zero covariance of pixels on the same scan circle shows the presence of striping. The factor of 2 in the variance of $T_i$ shows that this method has lost the putative $\sqrt{2}$ advantage of one-horned systems.

How can the $\sqrt{2}$ be recovered? A better baseline estimator is needed. For this white noise case, the average of all the noises in a scan circle is the optimum baseline estimator. But we don't have the noises – we only measure samples which are the sum of noise plus sky. Therefore we need to do any iterative solution to find the baseline:

1. subtract the signal from the scan using an estimate of the map,

2. compute the optimum baseline estimate, and

3. use the signal minus baseline to construct a new estimate of the map.

This procedure is almost identical to the time-ordered iterative approach used in Wright, Hinshaw & Bennett (1996). The only difference is that for differential data the contribution of the map to the "baseline" is just minus the sky temperature in the reference beam.

If applied to a model with $N/2$ scans of $N$ pixels crossing only at the NEP and SEP, the optimum approach reduces the sensitivity loss to a factor of $\sqrt{3/2}$ compared to an ideal total power system in the large $N$ limit. For large $N$, the difference between the NEP and SEP is determined to great precision, so the only significant terms in the covariance matrix are

$$
\begin{aligned}
\langle T_i T_i \rangle &= \frac{3}{2}\sigma_1^2 \\
\langle T_i T_j \rangle &= \begin{cases} \frac{1}{2}\sigma_1^2, & \text{if on the same scan;} \\ 0, & \text{otherwise.} \end{cases}
\end{aligned}
\tag{6}
$$

$$\tag{7}$$

This still has stripes, but both the noise and striping are reduced. In a real sky map, the number of multiply observed pixels in the polar caps is quite large, so the both the excess noise and the striping are reduced even more. This approach of subtracting an optimal baseline after correcting the baseline iteratively for the effect of the map on the baseline is equivalent to the method of adjusting the baselines in each scan circle using the set of overlapping pixels that was used by *FIRS* (Meyer, Cheng & Page 1991) and is planned by *COBRAS/SAMBA* (Bersanelli *et al.* 1996).
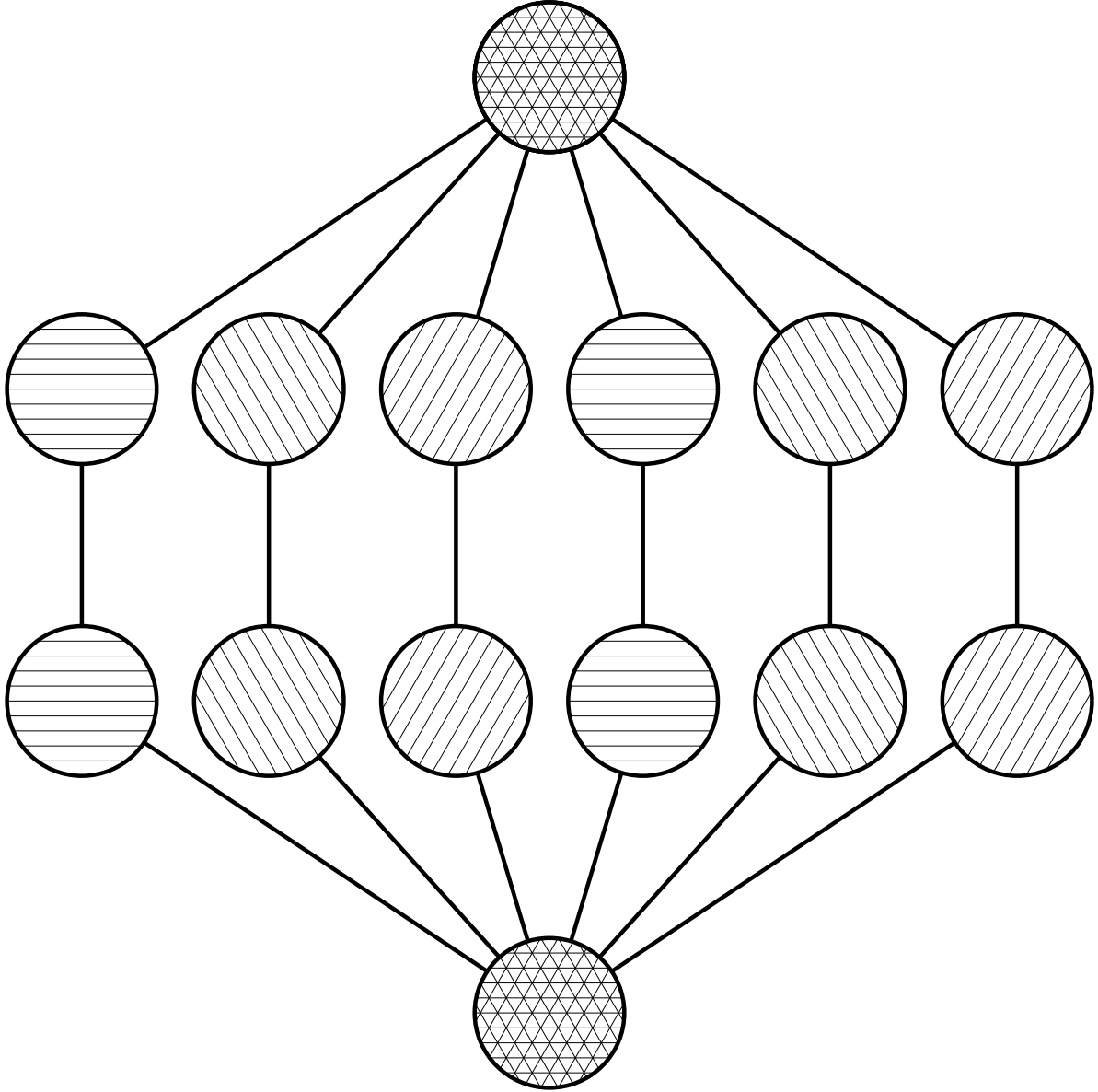
Fig. 1.— The toy sky model with 14 pixels observed in 3 scan circles, shown with different cross-hatching, totaling 18 data points.

### 3.  Toy Model

To illustrate the operations in the map-making process, I will use a toy model of the sky. This toy model has $N/2$ scans each with $N$ pixels crossing only at the NEP (North Ecliptic Pole) and SEP. Figure 1 shows the toy model with $N = 6$, so there are $n_d = N^2/2 = 18$ data points and $n_p = (N/2)(N-2) + 2 = 14$ pixels.

The pixel observed during each data sample must be known. Let $p(j)$ be the pixel observed during the $j^{th}$ data sample. I can write this as a matrix by defining $\mathbf{P}$ to be an $n_d \times n_p$ matrix, with 1 row for each observation and 1 column for each pixel. $\mathbf{P}$ is all zero except for a single "1" in each row at the column observed for that row's datum. Note that $\mathbf{P}$ is the operation of "flying the mission through a skymap" and that $\mathbf{P}$ maps a skymap into a data stream. The matrix $\mathbf{P}$ for the toy model with $N = 6$ is given by

$$\mathbf{P} = \begin{pmatrix}
1 & 0 & 0 & 0 & 0 & 0 & 0 & 0 & 0 & 0 & 0 & 0 & 0 & 0 \\
0 & 1 & 0 & 0 & 0 & 0 & 0 & 0 & 0 & 0 & 0 & 0 & 0 & 0 \\
0 & 0 & 1 & 0 & 0 & 0 & 0 & 0 & 0 & 0 & 0 & 0 & 0 & 0 \\
0 & 0 & 0 & 0 & 0 & 0 & 0 & 0 & 0 & 0 & 0 & 0 & 0 & 1 \\
0 & 0 & 0 & 1 & 0 & 0 & 0 & 0 & 0 & 0 & 0 & 0 & 0 & 0 \\
0 & 0 & 0 & 0 & 1 & 0 & 0 & 0 & 0 & 0 & 0 & 0 & 0 & 0 \\
1 & 0 & 0 & 0 & 0 & 0 & 0 & 0 & 0 & 0 & 0 & 0 & 0 & 0 \\
0 & 0 & 0 & 0 & 0 & 1 & 0 & 0 & 0 & 0 & 0 & 0 & 0 & 0 \\
0 & 0 & 0 & 0 & 0 & 0 & 1 & 0 & 0 & 0 & 0 & 0 & 0 & 0 \\
0 & 0 & 0 & 0 & 0 & 0 & 0 & 0 & 0 & 0 & 0 & 0 & 0 & 1 \\
0 & 0 & 0 & 0 & 0 & 0 & 0 & 1 & 0 & 0 & 0 & 0 & 0 & 0 \\
0 & 0 & 0 & 0 & 0 & 0 & 0 & 0 & 1 & 0 & 0 & 0 & 0 & 0 \\
1 & 0 & 0 & 0 & 0 & 0 & 0 & 0 & 0 & 0 & 0 & 0 & 0 & 0 \\
0 & 0 & 0 & 0 & 0 & 0 & 0 & 0 & 0 & 1 & 0 & 0 & 0 & 0 \\
0 & 0 & 0 & 0 & 0 & 0 & 0 & 0 & 0 & 0 & 1 & 0 & 0 & 0 \\
0 & 0 & 0 & 0 & 0 & 0 & 0 & 0 & 0 & 0 & 0 & 0 & 0 & 1 \\
0 & 0 & 0 & 0 & 0 & 0 & 0 & 0 & 0 & 0 & 0 & 1 & 0 & 0 \\
0 & 0 & 0 & 0 & 0 & 0 & 0 & 0 & 0 & 0 & 0 & 0 & 1 & 0
\end{pmatrix} \tag{8}$$

The NEP is pixel 1, the SEP is pixel 14, and scan circle 1 is pixels 1, 2, 3, 14, 4, 5 in order, while scan circle 2 is pixels 1, 6, 7, 14, 8, 9.

Define the matrix $\mathbf{W}$ to be an $n_d \times n_d$ matrix that corrects the data for the optimal baseline.

For the white noise case of the toy model, this matrix is given by

$$
\mathbf{W} = \frac{1}{5}
\begin{pmatrix}
5 & -1 & -1 & -1 & -1 & -1 & 0 & 0 & 0 & 0 & 0 & 0 & 0 & 0 & 0 & 0 & 0 & 0 \\
-1 & 5 & -1 & -1 & -1 & -1 & 0 & 0 & 0 & 0 & 0 & 0 & 0 & 0 & 0 & 0 & 0 & 0 \\
-1 & -1 & 5 & -1 & -1 & -1 & 0 & 0 & 0 & 0 & 0 & 0 & 0 & 0 & 0 & 0 & 0 & 0 \\
-1 & -1 & -1 & 5 & -1 & -1 & 0 & 0 & 0 & 0 & 0 & 0 & 0 & 0 & 0 & 0 & 0 & 0 \\
-1 & -1 & -1 & -1 & 5 & -1 & 0 & 0 & 0 & 0 & 0 & 0 & 0 & 0 & 0 & 0 & 0 & 0 \\
-1 & -1 & -1 & -1 & -1 & 5 & 0 & 0 & 0 & 0 & 0 & 0 & 0 & 0 & 0 & 0 & 0 & 0 \\
0 & 0 & 0 & 0 & 0 & 0 & 5 & -1 & -1 & -1 & -1 & -1 & 0 & 0 & 0 & 0 & 0 & 0 \\
0 & 0 & 0 & 0 & 0 & 0 & -1 & 5 & -1 & -1 & -1 & -1 & 0 & 0 & 0 & 0 & 0 & 0 \\
0 & 0 & 0 & 0 & 0 & 0 & -1 & -1 & 5 & -1 & -1 & -1 & 0 & 0 & 0 & 0 & 0 & 0 \\
0 & 0 & 0 & 0 & 0 & 0 & -1 & -1 & -1 & 5 & -1 & -1 & 0 & 0 & 0 & 0 & 0 & 0 \\
0 & 0 & 0 & 0 & 0 & 0 & -1 & -1 & -1 & -1 & 5 & -1 & 0 & 0 & 0 & 0 & 0 & 0 \\
0 & 0 & 0 & 0 & 0 & 0 & -1 & -1 & -1 & -1 & -1 & 5 & 0 & 0 & 0 & 0 & 0 & 0 \\
0 & 0 & 0 & 0 & 0 & 0 & 0 & 0 & 0 & 0 & 0 & 0 & 5 & -1 & -1 & -1 & -1 & -1 \\
0 & 0 & 0 & 0 & 0 & 0 & 0 & 0 & 0 & 0 & 0 & 0 & -1 & 5 & -1 & -1 & -1 & -1 \\
0 & 0 & 0 & 0 & 0 & 0 & 0 & 0 & 0 & 0 & 0 & 0 & -1 & -1 & 5 & -1 & -1 & -1 \\
0 & 0 & 0 & 0 & 0 & 0 & 0 & 0 & 0 & 0 & 0 & 0 & -1 & -1 & -1 & 5 & -1 & -1 \\
0 & 0 & 0 & 0 & 0 & 0 & 0 & 0 & 0 & 0 & 0 & 0 & -1 & -1 & -1 & -1 & 5 & -1 \\
0 & 0 & 0 & 0 & 0 & 0 & 0 & 0 & 0 & 0 & 0 & 0 & -1 & -1 & -1 & -1 & -1 & 5
\end{pmatrix}
\tag{9}
$$

The matrix $\mathbf{W}$ is the $n_d \times n_d$ matrix that applies the optimal baseline correction. Then for an observed data stream $\mathbf{S}$, the desired map is the $\mathbf{T}$ that best satisfies the $n_d$ equations:

$$
\mathbf{WPT} = \mathbf{WS}
\tag{10}
$$

The application of $\mathbf{W}$ to $\mathbf{S}$ makes the elements of the right hand side uncorrelated. Actually there is still an $\mathcal{O}(1/N)$ correlation because the true mean of the scan is completely undetermined, but I will ignore this effect which is negligible for real CMB experiments. Let $\sigma$ be the standard deviation of the noise in these values, which I will take to be $\sigma = 1$ in the following examples. Note that this implies that the standard deviation of the original data is somewhat less than one due to the variance introduced by baseline subtraction. Proceeding in the normal least squares fashion, make $n_p$ normal equations:

$$
\mathbf{P}^T \mathbf{W}^T \frac{1}{\sigma^2} \mathbf{WPT} = \mathbf{P}^T \mathbf{W}^T \frac{1}{\sigma^2} \mathbf{WS}
\tag{11}
$$

The matrix $\mathbf{P}^T$ is the operation of "summing a data stream into pixels". Thus the $n_p \times 1$ right hand side is

$$
\mathbf{B} = \mathbf{P}^T \mathbf{W}^T \frac{1}{\sigma^2} \mathbf{WS}
$$

and the $n_p \times n_p$ correlation matrix is

$$
\mathbf{A} = \mathbf{P}^T \mathbf{W}^T \frac{1}{\sigma^2} \mathbf{WP}
$$

and the equation to solve is

$$
\mathbf{AT} = \mathbf{B}
\tag{12}
$$

For large problems this should be solved iteratively, and only products of the form $\mathbf{A}$ times a vector are needed.

However, for the toy model $\mathbf{A}^{-1}$ can be computed directly. Of course, $\mathbf{A}$ is singular so an extra equation stating that the sum of the map is zero must be added to the $n_d$ equations from the observations. This adds the matrix $\mathbf{1}$ which is matrix with all elements equal to unity to $\mathbf{A}$. Do not confuse $\mathbf{1}$ with the identity matrix $\mathbf{I}$. The generalized inverse of $\mathbf{A}$ is then given by

$$\mathbf{A}^{-1} = (\mathbf{A} + \mathbf{1})^{-1} - n_p^{-2}\mathbf{1}. \tag{13}$$

This particular form for the generalized inverse is a special case that only fixes the zero eigenvalue associated with the mean of the map. For experiments with partial sky coverage or disconnected regions the more general form of the generalized inverse should be used:

$$\mathbf{A}^{-1} \approx \lim_{\epsilon \to 0^+} (\mathbf{A} + \epsilon \mathbf{I})^{-1}. \tag{14}$$

When solving $\mathbf{AX} = \mathbf{Y}$ be sure that $\mathbf{Y}$ is orthogonal to all the eigenvectors of $\mathbf{A}$ with zero eigenvalues. For the toy model

$$\mathbf{A} = \frac{1}{25} \begin{pmatrix}
90 & -6 & -6 & -6 & -6 & -6 & -6 & -6 & -6 & -6 & -6 & -6 & -6 & -18 \\
-6 & 30 & -6 & -6 & -6 & 0 & 0 & 0 & 0 & 0 & 0 & 0 & 0 & -6 \\
-6 & -6 & 30 & -6 & -6 & 0 & 0 & 0 & 0 & 0 & 0 & 0 & 0 & -6 \\
-6 & -6 & -6 & 30 & -6 & 0 & 0 & 0 & 0 & 0 & 0 & 0 & 0 & -6 \\
-6 & -6 & -6 & -6 & 30 & 0 & 0 & 0 & 0 & 0 & 0 & 0 & 0 & -6 \\
-6 & 0 & 0 & 0 & 0 & 30 & -6 & -6 & -6 & 0 & 0 & 0 & 0 & -6 \\
-6 & 0 & 0 & 0 & 0 & -6 & 30 & -6 & -6 & 0 & 0 & 0 & 0 & -6 \\
-6 & 0 & 0 & 0 & 0 & -6 & -6 & 30 & -6 & 0 & 0 & 0 & 0 & -6 \\
-6 & 0 & 0 & 0 & 0 & -6 & -6 & -6 & 30 & 0 & 0 & 0 & 0 & -6 \\
-6 & 0 & 0 & 0 & 0 & 0 & 0 & 0 & 0 & 30 & -6 & -6 & -6 & -6 \\
-6 & 0 & 0 & 0 & 0 & 0 & 0 & 0 & 0 & -6 & 30 & -6 & -6 & -6 \\
-6 & 0 & 0 & 0 & 0 & 0 & 0 & 0 & 0 & -6 & -6 & 30 & -6 & -6 \\
-6 & 0 & 0 & 0 & 0 & 0 & 0 & 0 & 0 & -6 & -6 & -6 & 30 & -6 \\
-18 & -6 & -6 & -6 & -6 & -6 & -6 & -6 & -6 & -6 & -6 & -6 & -6 & 90
\end{pmatrix} \tag{15}$$

The covariance matrix is given by $\mathbf{A}^{-1} =$

$$\begin{pmatrix}
0.24 & -0.02 & -0.02 & -0.02 & -0.02 & -0.02 & -0.02 & -0.02 & -0.02 & -0.02 & -0.02 & -0.02 & -0.02 & 0.01 \\
-0.02 & 0.87 & 0.18 & 0.18 & 0.18 & -0.17 & -0.17 & -0.17 & -0.17 & -0.17 & -0.17 & -0.17 & -0.17 & -0.02 \\
-0.02 & 0.18 & 0.87 & 0.18 & 0.18 & -0.17 & -0.17 & -0.17 & -0.17 & -0.17 & -0.17 & -0.17 & -0.17 & -0.02 \\
-0.02 & 0.18 & 0.18 & 0.87 & 0.18 & -0.17 & -0.17 & -0.17 & -0.17 & -0.17 & -0.17 & -0.17 & -0.17 & -0.02 \\
-0.02 & 0.18 & 0.18 & 0.18 & 0.87 & -0.17 & -0.17 & -0.17 & -0.17 & -0.17 & -0.17 & -0.17 & -0.17 & -0.02 \\
-0.02 & -0.17 & -0.17 & -0.17 & -0.17 & 0.87 & 0.18 & 0.18 & 0.18 & -0.17 & -0.17 & -0.17 & -0.17 & -0.02 \\
-0.02 & -0.17 & -0.17 & -0.17 & -0.17 & 0.18 & 0.87 & 0.18 & 0.18 & -0.17 & -0.17 & -0.17 & -0.17 & -0.02 \\
-0.02 & -0.17 & -0.17 & -0.17 & -0.17 & 0.18 & 0.18 & 0.87 & 0.18 & -0.17 & -0.17 & -0.17 & -0.17 & -0.02 \\
-0.02 & -0.17 & -0.17 & -0.17 & -0.17 & 0.18 & 0.18 & 0.18 & 0.87 & -0.17 & -0.17 & -0.17 & -0.17 & -0.02 \\
-0.02 & -0.17 & -0.17 & -0.17 & -0.17 & -0.17 & -0.17 & -0.17 & -0.17 & 0.87 & 0.18 & 0.18 & 0.18 & -0.02 \\
-0.02 & -0.17 & -0.17 & -0.17 & -0.17 & -0.17 & -0.17 & -0.17 & -0.17 & 0.18 & 0.87 & 0.18 & 0.18 & -0.02 \\
-0.02 & -0.17 & -0.17 & -0.17 & -0.17 & -0.17 & -0.17 & -0.17 & -0.17 & 0.18 & 0.18 & 0.87 & 0.18 & -0.02 \\
-0.02 & -0.17 & -0.17 & -0.17 & -0.17 & -0.17 & -0.17 & -0.17 & -0.17 & 0.18 & 0.18 & 0.18 & 0.87 & -0.02 \\
0.01 & -0.02 & -0.02 & -0.02 & -0.02 & -0.02 & -0.02 & -0.02 & -0.02 & -0.02 & -0.02 & -0.02 & -0.02 & 0.24
\end{pmatrix}$$

Note that this particular form of the generalized inverse gives a zero sum for each row of $\mathbf{A}^{-1}$ and this introduces the anti-correlation for points on different scan circles.
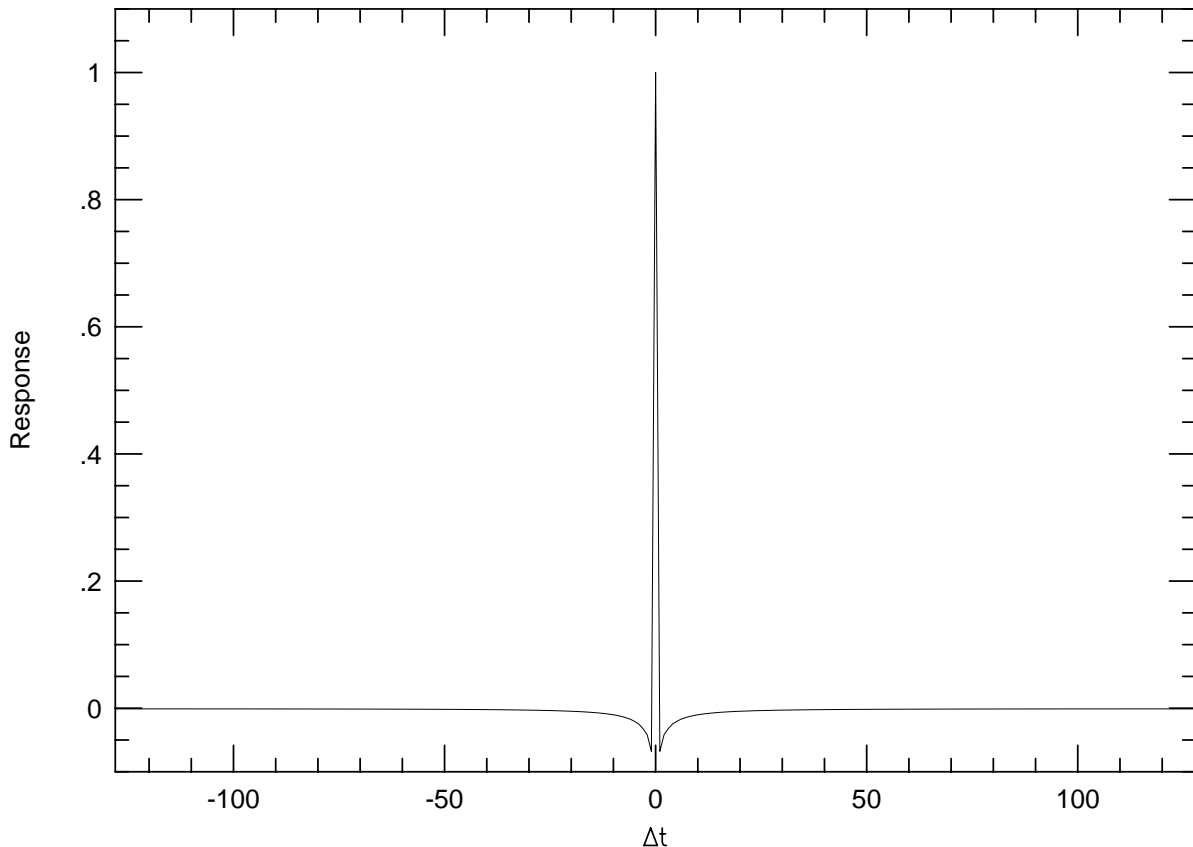
Fig. 2.— The pre-whitening filter for $f_K = 10 f_{spin}$ with 256 points per spin.

## 4. $1/f$ Noise

Most instruments do not produce white noise, but have slow drifts and other anomalies that produce an excess noise at low frequencies in the output. The unknown baseline for each scan circle in the toy model used earlier is an example of low frequency noise: it corresponds to a $\delta(f)$ spike in the noise power spectrum at zero frequency. Real instruments have this zero frequency spike, but they also usually have a more gradual rise in the noise power spectrum as $f \to 0$. Typically an excess noise varying like $1/f$ is seen, giving a noise power spectrum

$$P(f) = 2\Delta t\, \sigma_1^2 \left(1 + \frac{f_K}{f}\right) \tag{16}$$

where $\Delta t$ is the sampling interval, $\sigma_1$ is the noise in one sample ignoring the $1/f$ term, and $f_K$ is the $1/f$ "knee" frequency.

In a spin-scanned system, $1/f$ noise is only important if the spin rate is less than $f_K$. For *COBRAS/SAMBA* the spin rate should be faster than the output drifts in either the bolometers or the differencing HEMTs. But in balloon-borne experiments, drifts in the atmosphere will produce excess low frequency noise that must be correctly treated during data analysis.

In the presence of $1/f$ noise, successive samples of the signal are correlated. In order to
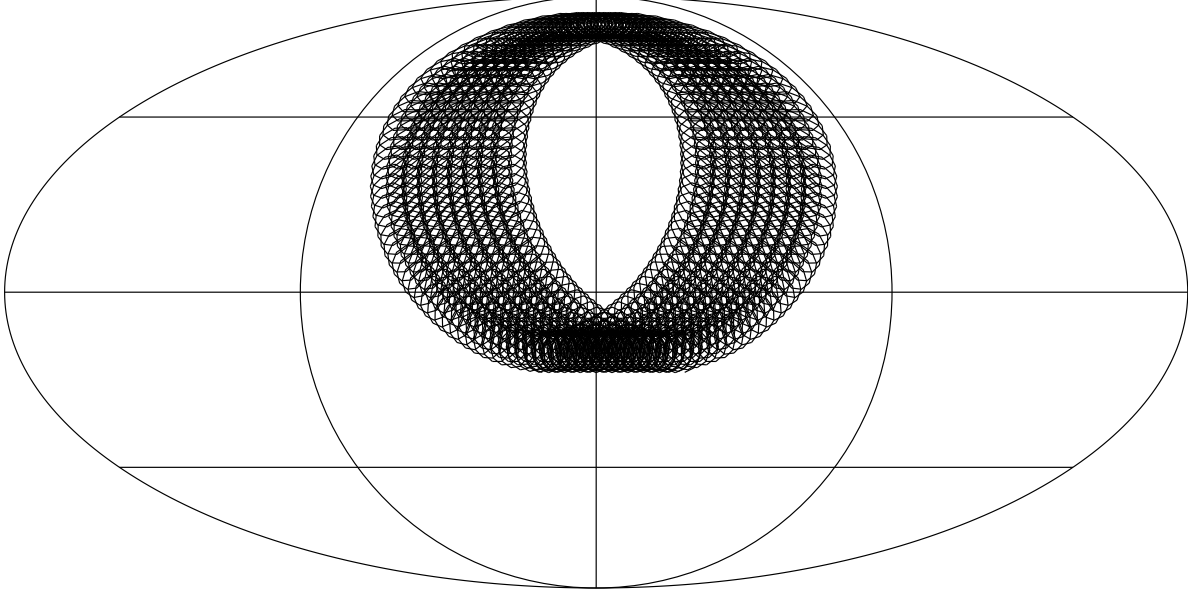
# UCSB Scan Path



Fig. 3.— A complex scan pattern with a 10° circular scan superimposed on rotation around the zenith and the diurnal rate.

simplify the analysis, a "pre-whitening" filter with transmission

$$W(f) = \sqrt{\frac{f}{f + f_K}} \tag{17}$$

should be applied. After applying this filter, the noise in different samples will be uncorrelated. The impulse response function of $W(f)$ in the time domain will integrate to zero because the response of $W(f)$ vanishes for $f = 0$. The impulse response function $W(t)$ will have a $\delta(t)$ spike at zero time because $W(f) \to 1$ as $f \to \infty$. Thus the action of $W$ is to replace the signal stream with signal minus baseline, and the baseline used is the optimal baseline estimator. Figure 2 show the pre-whitening filter for $f_K = 10 f_{spin}$.

While the noise in the output of $W$ is uncorrelated, this filter makes each observation depend on many sky values. For a discretely sampled data, the $W$ in the time domain is given by a vector of weights $W_k$, where $W_0 = 1$ and $\sum W_k = 0$. For *post facto* data analysis the time symmetric filter with $W_{-k} = W_k$ can be used instead of a causal filter.

In terms of the matrices introduced earlier, only $\mathbf{W}$ needs to be changed for $1/f$ noise. In the toy model, the scan circles are so short that only a very short pre-whitening filter can be used, so
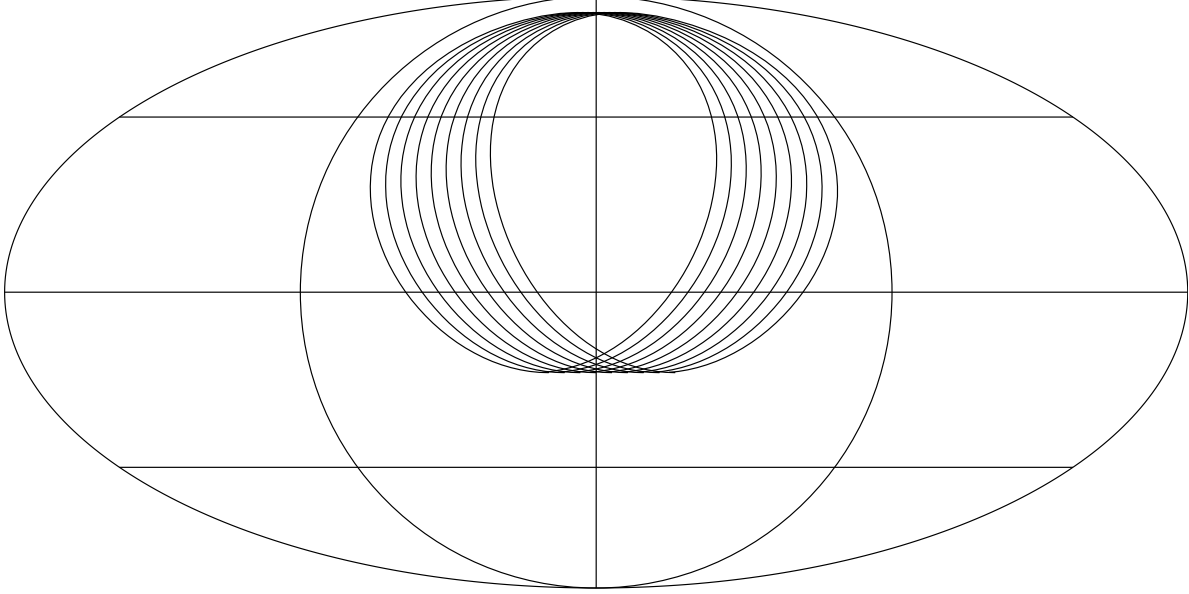
# FIRS Scan Path



Fig. 4.— A simple scan pattern generated by rotation around the zenith and the diurnal rate.

I will use $W_k = -0.5, 1, \& -0.5$. This gives

$$\mathbf{W} = \frac{1}{2}\begin{pmatrix}
2 & -1 & 0 & 0 & 0 & -1 & 0 & 0 & 0 & 0 & 0 & 0 & 0 & 0 & 0 & 0 & 0 & 0 \\
-1 & 2 & -1 & 0 & 0 & 0 & 0 & 0 & 0 & 0 & 0 & 0 & 0 & 0 & 0 & 0 & 0 & 0 \\
0 & -1 & 2 & -1 & 0 & 0 & 0 & 0 & 0 & 0 & 0 & 0 & 0 & 0 & 0 & 0 & 0 & 0 \\
0 & 0 & -1 & 2 & -1 & 0 & 0 & 0 & 0 & 0 & 0 & 0 & 0 & 0 & 0 & 0 & 0 & 0 \\
0 & 0 & 0 & -1 & 2 & -1 & 0 & 0 & 0 & 0 & 0 & 0 & 0 & 0 & 0 & 0 & 0 & 0 \\
-1 & 0 & 0 & 0 & -1 & 2 & 0 & 0 & 0 & 0 & 0 & 0 & 0 & 0 & 0 & 0 & 0 & 0 \\
0 & 0 & 0 & 0 & 0 & 0 & 2 & -1 & 0 & 0 & 0 & -1 & 0 & 0 & 0 & 0 & 0 & 0 \\
0 & 0 & 0 & 0 & 0 & 0 & -1 & 2 & -1 & 0 & 0 & 0 & 0 & 0 & 0 & 0 & 0 & 0 \\
0 & 0 & 0 & 0 & 0 & 0 & 0 & -1 & 2 & -1 & 0 & 0 & 0 & 0 & 0 & 0 & 0 & 0 \\
0 & 0 & 0 & 0 & 0 & 0 & 0 & 0 & -1 & 2 & -1 & 0 & 0 & 0 & 0 & 0 & 0 & 0 \\
0 & 0 & 0 & 0 & 0 & 0 & 0 & 0 & 0 & -1 & 2 & -1 & 0 & 0 & 0 & 0 & 0 & 0 \\
0 & 0 & 0 & 0 & 0 & 0 & -1 & 0 & 0 & 0 & -1 & 2 & 0 & 0 & 0 & 0 & 0 & 0 \\
0 & 0 & 0 & 0 & 0 & 0 & 0 & 0 & 0 & 0 & 0 & 0 & 2 & -1 & 0 & 0 & 0 & -1 \\
0 & 0 & 0 & 0 & 0 & 0 & 0 & 0 & 0 & 0 & 0 & 0 & -1 & 2 & -1 & 0 & 0 & 0 \\
0 & 0 & 0 & 0 & 0 & 0 & 0 & 0 & 0 & 0 & 0 & 0 & 0 & -1 & 2 & -1 & 0 & 0 \\
0 & 0 & 0 & 0 & 0 & 0 & 0 & 0 & 0 & 0 & 0 & 0 & 0 & 0 & -1 & 2 & -1 & 0 \\
0 & 0 & 0 & 0 & 0 & 0 & 0 & 0 & 0 & 0 & 0 & 0 & 0 & 0 & 0 & -1 & 2 & -1 \\
0 & 0 & 0 & 0 & 0 & 0 & 0 & 0 & 0 & 0 & 0 & 0 & -1 & 0 & 0 & 0 & -1 & 2
\end{pmatrix} \tag{18}$$

The correlation matrix is

$$\mathbf{A} = \frac{1}{4}
\begin{pmatrix}
18 & -4 & 1 & 1 & -4 & -4 & 1 & 1 & -4 & -4 & 1 & 1 & -4 & 0 \\
-4 & 6 & -4 & 0 & 1 & 0 & 0 & 0 & 0 & 0 & 0 & 0 & 0 & 1 \\
1 & -4 & 6 & 1 & 0 & 0 & 0 & 0 & 0 & 0 & 0 & 0 & 0 & -4 \\
1 & 0 & 1 & 6 & -4 & 0 & 0 & 0 & 0 & 0 & 0 & 0 & 0 & -4 \\
-4 & 1 & 0 & -4 & 6 & 0 & 0 & 0 & 0 & 0 & 0 & 0 & 0 & 1 \\
-4 & 0 & 0 & 0 & 0 & 6 & -4 & 0 & 1 & 0 & 0 & 0 & 0 & 1 \\
1 & 0 & 0 & 0 & 0 & -4 & 6 & 1 & 0 & 0 & 0 & 0 & 0 & -4 \\
1 & 0 & 0 & 0 & 0 & 0 & 1 & 6 & -4 & 0 & 0 & 0 & 0 & -4 \\
-4 & 0 & 0 & 0 & 0 & 1 & 0 & -4 & 6 & 0 & 0 & 0 & 0 & 1 \\
-4 & 0 & 0 & 0 & 0 & 0 & 0 & 0 & 0 & 6 & -4 & 0 & 1 & 1 \\
1 & 0 & 0 & 0 & 0 & 0 & 0 & 0 & 0 & -4 & 6 & 1 & 0 & -4 \\
1 & 0 & 0 & 0 & 0 & 0 & 0 & 0 & 0 & 0 & 1 & 6 & -4 & -4 \\
-4 & 0 & 0 & 0 & 0 & 0 & 0 & 0 & 0 & 1 & 0 & -4 & 6 & 1 \\
0 & 1 & -4 & -4 & 1 & 1 & -4 & -4 & 1 & 1 & -4 & -4 & 1 & 18
\end{pmatrix}
\tag{19}$$

The covariance matrix is given by $\mathbf{A}^{-1} =$

$$
\begin{pmatrix}
0.54 & 0.19 & -0.22 & -0.22 & 0.19 & 0.19 & -0.22 & -0.22 & 0.19 & 0.19 & -0.22 & -0.22 & 0.19 & -0.38 \\
0.19 & 1.52 & 0.93 & -0.85 & -0.70 & -0.01 & -0.20 & -0.20 & -0.01 & -0.01 & -0.20 & -0.20 & -0.01 & -0.22 \\
-0.22 & 0.93 & 1.52 & -0.70 & -0.85 & -0.20 & -0.01 & -0.01 & -0.20 & -0.20 & -0.01 & -0.01 & -0.20 & 0.19 \\
-0.22 & -0.85 & -0.70 & 1.52 & 0.93 & -0.20 & -0.01 & -0.01 & -0.20 & -0.20 & -0.01 & -0.01 & -0.20 & 0.19 \\
0.19 & -0.70 & -0.85 & 0.93 & 1.52 & -0.01 & -0.20 & -0.20 & -0.01 & -0.01 & -0.20 & -0.20 & -0.01 & -0.22 \\
0.19 & -0.01 & -0.20 & -0.20 & -0.01 & 1.52 & 0.93 & -0.85 & -0.70 & -0.01 & -0.20 & -0.20 & -0.01 & -0.22 \\
-0.22 & -0.20 & -0.01 & -0.01 & -0.20 & 0.93 & 1.52 & -0.70 & -0.85 & -0.20 & -0.01 & -0.01 & -0.20 & 0.19 \\
-0.22 & -0.20 & -0.01 & -0.01 & -0.20 & -0.85 & -0.70 & 1.52 & 0.93 & -0.20 & -0.01 & -0.01 & -0.20 & 0.19 \\
0.19 & -0.01 & -0.20 & -0.20 & -0.01 & -0.70 & -0.85 & 0.93 & 1.52 & -0.01 & -0.20 & -0.20 & -0.01 & -0.22 \\
0.19 & -0.01 & -0.20 & -0.20 & -0.01 & -0.01 & -0.20 & -0.20 & -0.01 & 1.52 & 0.93 & -0.85 & -0.70 & -0.22 \\
-0.22 & -0.20 & -0.01 & -0.01 & -0.20 & -0.20 & -0.01 & -0.01 & -0.20 & 0.93 & 1.52 & -0.70 & -0.85 & 0.19 \\
-0.22 & -0.20 & -0.01 & -0.01 & -0.20 & -0.20 & -0.01 & -0.01 & -0.20 & -0.85 & -0.70 & 1.52 & 0.93 & 0.19 \\
0.19 & -0.01 & -0.20 & -0.20 & -0.01 & -0.01 & -0.20 & -0.20 & -0.01 & -0.70 & -0.85 & 0.93 & 1.52 & -0.22 \\
-0.38 & -0.22 & 0.19 & 0.19 & -0.22 & -0.22 & 0.19 & 0.19 & -0.22 & -0.22 & 0.19 & 0.19 & -0.22 & 0.54
\end{pmatrix}
$$

## 5. Continuous Scanning

The examples so far are based on scanning in discrete scan circles. But continuous scanning is also possible. With a continuous scan $\mathbf{W}$ changes to

$$\mathbf{W} = \frac{1}{2}\begin{pmatrix}
2 & -1 & 0 & 0 & 0 & 0 & 0 & 0 & 0 & 0 & 0 & 0 & 0 & 0 & 0 & 0 & 0 & -1 \\
-1 & 2 & -1 & 0 & 0 & 0 & 0 & 0 & 0 & 0 & 0 & 0 & 0 & 0 & 0 & 0 & 0 & 0 \\
0 & -1 & 2 & -1 & 0 & 0 & 0 & 0 & 0 & 0 & 0 & 0 & 0 & 0 & 0 & 0 & 0 & 0 \\
0 & 0 & -1 & 2 & -1 & 0 & 0 & 0 & 0 & 0 & 0 & 0 & 0 & 0 & 0 & 0 & 0 & 0 \\
0 & 0 & 0 & -1 & 2 & -1 & 0 & 0 & 0 & 0 & 0 & 0 & 0 & 0 & 0 & 0 & 0 & 0 \\
0 & 0 & 0 & 0 & -1 & 2 & -1 & 0 & 0 & 0 & 0 & 0 & 0 & 0 & 0 & 0 & 0 & 0 \\
0 & 0 & 0 & 0 & 0 & -1 & 2 & -1 & 0 & 0 & 0 & 0 & 0 & 0 & 0 & 0 & 0 & 0 \\
0 & 0 & 0 & 0 & 0 & 0 & -1 & 2 & -1 & 0 & 0 & 0 & 0 & 0 & 0 & 0 & 0 & 0 \\
0 & 0 & 0 & 0 & 0 & 0 & 0 & -1 & 2 & -1 & 0 & 0 & 0 & 0 & 0 & 0 & 0 & 0 \\
0 & 0 & 0 & 0 & 0 & 0 & 0 & 0 & -1 & 2 & -1 & 0 & 0 & 0 & 0 & 0 & 0 & 0 \\
0 & 0 & 0 & 0 & 0 & 0 & 0 & 0 & 0 & -1 & 2 & -1 & 0 & 0 & 0 & 0 & 0 & 0 \\
0 & 0 & 0 & 0 & 0 & 0 & 0 & 0 & 0 & 0 & -1 & 2 & -1 & 0 & 0 & 0 & 0 & 0 \\
0 & 0 & 0 & 0 & 0 & 0 & 0 & 0 & 0 & 0 & 0 & -1 & 2 & -1 & 0 & 0 & 0 & 0 \\
0 & 0 & 0 & 0 & 0 & 0 & 0 & 0 & 0 & 0 & 0 & 0 & -1 & 2 & -1 & 0 & 0 & 0 \\
0 & 0 & 0 & 0 & 0 & 0 & 0 & 0 & 0 & 0 & 0 & 0 & 0 & -1 & 2 & -1 & 0 & 0 \\
0 & 0 & 0 & 0 & 0 & 0 & 0 & 0 & 0 & 0 & 0 & 0 & 0 & 0 & -1 & 2 & -1 & 0 \\
0 & 0 & 0 & 0 & 0 & 0 & 0 & 0 & 0 & 0 & 0 & 0 & 0 & 0 & 0 & -1 & 2 & -1 \\
-1 & 0 & 0 & 0 & 0 & 0 & 0 & 0 & 0 & 0 & 0 & 0 & 0 & 0 & 0 & 0 & -1 & 2
\end{pmatrix} \tag{20}$$

and the correlation matrix changes to

$$\mathbf{A} = \frac{1}{4}\begin{pmatrix}
18 & -4 & 1 & 1 & -4 & -4 & 1 & 1 & -4 & -4 & 1 & 1 & -4 & 0 \\
-4 & 6 & -4 & 0 & 0 & 0 & 0 & 0 & 0 & 0 & 0 & 0 & 1 & 1 \\
1 & -4 & 6 & 1 & 0 & 0 & 0 & 0 & 0 & 0 & 0 & 0 & 0 & -4 \\
1 & 0 & 1 & 6 & -4 & 0 & 0 & 0 & 0 & 0 & 0 & 0 & 0 & -4 \\
-4 & 0 & 0 & -4 & 6 & 1 & 0 & 0 & 0 & 0 & 0 & 0 & 0 & 1 \\
-4 & 0 & 0 & 0 & 1 & 6 & -4 & 0 & 0 & 0 & 0 & 0 & 0 & 1 \\
1 & 0 & 0 & 0 & 0 & -4 & 6 & 1 & 0 & 0 & 0 & 0 & 0 & -4 \\
1 & 0 & 0 & 0 & 0 & 0 & 1 & 6 & -4 & 0 & 0 & 0 & 0 & -4 \\
-4 & 0 & 0 & 0 & 0 & 0 & 0 & -4 & 6 & 1 & 0 & 0 & 0 & 1 \\
-4 & 0 & 0 & 0 & 0 & 0 & 0 & 0 & 1 & 6 & -4 & 0 & 0 & 1 \\
1 & 0 & 0 & 0 & 0 & 0 & 0 & 0 & 0 & -4 & 6 & 1 & 0 & -4 \\
1 & 0 & 0 & 0 & 0 & 0 & 0 & 0 & 0 & 0 & 1 & 6 & -4 & -4 \\
-4 & 1 & 0 & 0 & 0 & 0 & 0 & 0 & 0 & 0 & 0 & -4 & 6 & 1 \\
0 & 1 & -4 & -4 & 1 & 1 & -4 & -4 & 1 & 1 & -4 & -4 & 1 & 18
\end{pmatrix} \tag{21}$$

The covariance matrix becomes $\mathbf{A}^{-1} =$

$$
\begin{pmatrix}
0.54 & 0.19 & -0.22 & -0.22 & 0.19 & 0.19 & -0.22 & -0.22 & 0.19 & 0.19 & -0.22 & -0.22 & 0.19 & -0.38 \\
0.19 & 1.38 & 0.78 & -0.51 & -0.23 & 0.06 & -0.15 & -0.23 & -0.05 & 0.06 & -0.10 & -0.51 & -0.45 & -0.22 \\
-0.22 & 0.78 & 1.38 & -0.45 & -0.51 & -0.10 & 0.06 & -0.05 & -0.23 & -0.15 & 0.06 & -0.23 & -0.51 & 0.19 \\
-0.22 & -0.51 & -0.45 & 1.38 & 0.78 & -0.51 & -0.23 & 0.06 & -0.15 & -0.23 & -0.05 & 0.06 & -0.10 & 0.19 \\
0.19 & -0.23 & -0.51 & 0.78 & 1.38 & -0.45 & -0.51 & -0.10 & 0.06 & -0.05 & -0.23 & -0.15 & 0.06 & -0.22 \\
0.19 & 0.06 & -0.10 & -0.51 & -0.45 & 1.38 & 0.78 & -0.51 & -0.23 & 0.06 & -0.15 & -0.23 & -0.05 & -0.22 \\
-0.22 & -0.15 & 0.06 & -0.23 & -0.51 & 0.78 & 1.38 & -0.45 & -0.51 & -0.10 & 0.06 & -0.05 & -0.23 & 0.19 \\
-0.22 & -0.23 & -0.05 & 0.06 & -0.10 & -0.51 & -0.45 & 1.38 & 0.78 & -0.51 & -0.23 & 0.06 & -0.15 & 0.19 \\
0.19 & -0.05 & -0.23 & -0.15 & 0.06 & -0.23 & -0.51 & 0.78 & 1.38 & -0.45 & -0.51 & -0.10 & 0.06 & -0.22 \\
0.19 & 0.06 & -0.15 & -0.23 & -0.05 & 0.06 & -0.10 & -0.51 & -0.45 & 1.38 & 0.78 & -0.51 & -0.23 & -0.22 \\
-0.22 & -0.10 & 0.06 & -0.05 & -0.23 & -0.15 & 0.06 & -0.23 & -0.51 & 0.78 & 1.38 & -0.45 & -0.51 & 0.19 \\
-0.22 & -0.51 & -0.23 & 0.06 & -0.15 & -0.23 & -0.05 & 0.06 & -0.10 & -0.51 & -0.45 & 1.38 & 0.78 & 0.19 \\
0.19 & -0.45 & -0.51 & -0.10 & 0.06 & -0.05 & -0.23 & -0.15 & 0.06 & -0.23 & -0.51 & 0.78 & 1.38 & -0.22 \\
-0.38 & -0.22 & 0.19 & 0.19 & -0.22 & -0.22 & 0.19 & 0.19 & -0.22 & -0.22 & 0.19 & 0.19 & -0.22 & 0.54
\end{pmatrix}
$$

which is slightly better than the scan circle case because the continuous scan introduces some new comparisons.

For large datasets and large maps, the actual construction of $\mathbf{A}$ and $\mathbf{A}^{-1}$ is impractical. However, the evaluation of $\mathbf{AX}$ for any vector $\mathbf{X}$ can be done in a reasonable amount of time by following these steps:
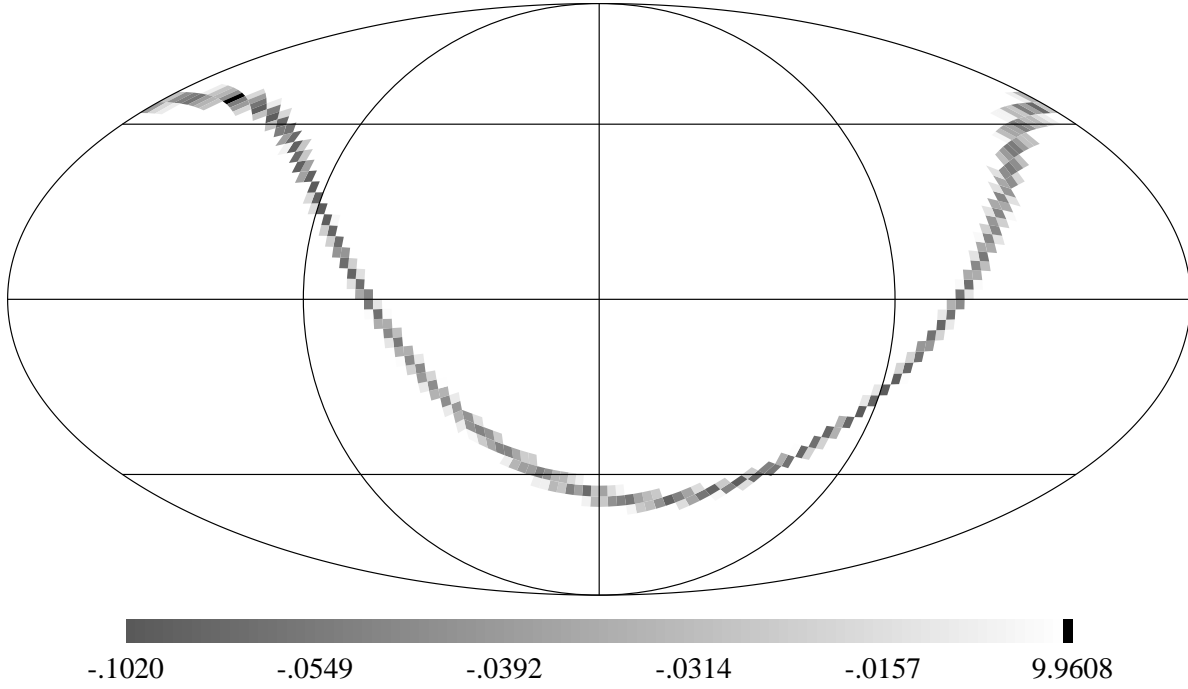
1. Apply $\mathbf{P}$: Fly the mission through the map, which takes $\mathcal{O}(n_d)$ operations.

2. Apply $\mathbf{W}^T\mathbf{W}$: This is a convolution. For the scan circle case, the convolution is done in $N$ sample blocks, and the total work is $\mathcal{O}(n_d \ln N)$ operations when using the FFT. For the continuously scanned case, the filter to be applied to the data is $\mathcal{O}(L_W)$ points long and the total work is $\mathcal{O}(n_d \ln L_W)$ when using FFTs.

3. Apply $\mathbf{P}^T$: Sum into pixels, which takes $\mathcal{O}(n_d)$ operations.

Thus the evaluation of $\mathbf{AX}$ takes $\mathcal{O}(n_d \ln L_W)$ operations and standard methods for the iterative solution of sparse systems that only need matrix-vector products can be used. This process should converge well for a complex scan pattern that crosses each pixel several times in different directions, such as the cycloidal scan produced by the scan plate in Lubin's balloon experiment, shown in Figure 3. A simple scan pattern such as rotating at constant elevation while the Earth turns, shown in Figure 4, will lead to much slower convergence of the iterations. Since pixels are always scanned in the same direction (unless the flight is long enough to see the sky both rising and setting), the simple scan pattern will give a final map with stripes.

## 6. Bigger Examples

These equations have been implemented for a bigger example using DMR pixels in galactic coordinates, and 256 scans through the ecliptic poles evenly spaced in ecliptic longitude, each scan having 256 points. Thus there are a total of $n_d = 256^2 = 65536$ observations for $n_p = 6144$ pixels. Since the whole matrices $\mathbf{A}$ or $\mathbf{A}^{-1}$ are too big to print out, I have made maps from a single row of these matrices. The pixel on the diagonal in this row is the Lockman Hole at $l = 150.5°$ and

# Row of Correlation Matrix with White Noise



| -.1020 | -.0549 | -.0392 | -.0314 | -.0157 | 9.9608 |

# Row of Covariance Matrix with White Noise
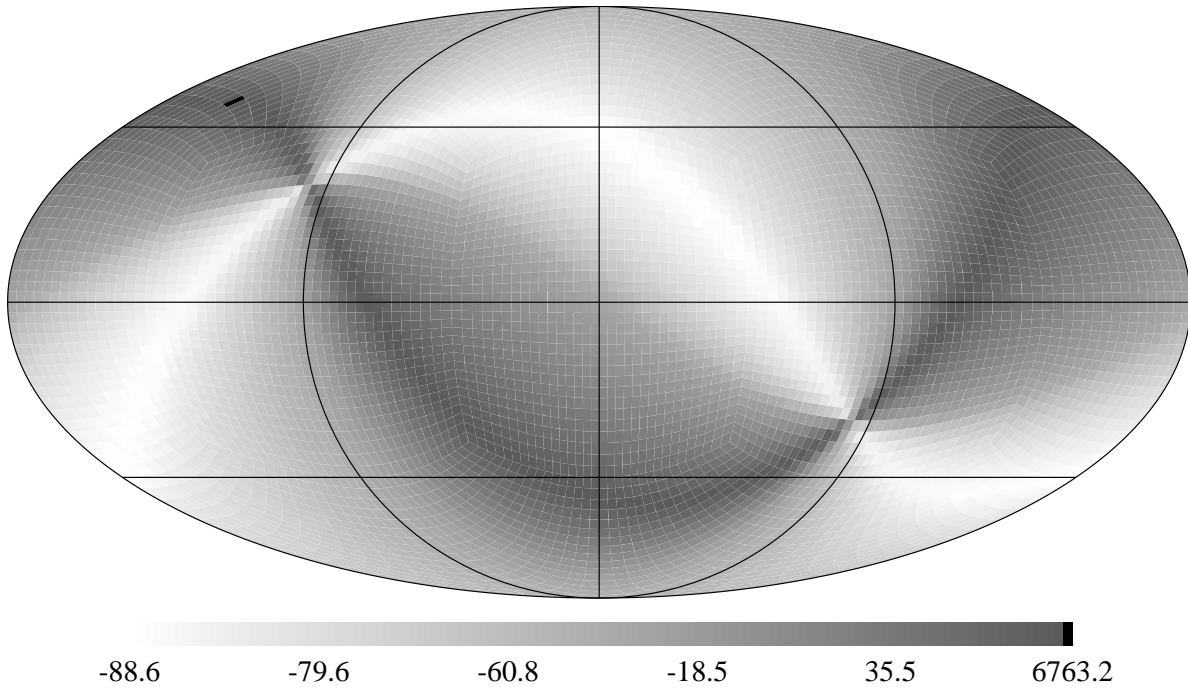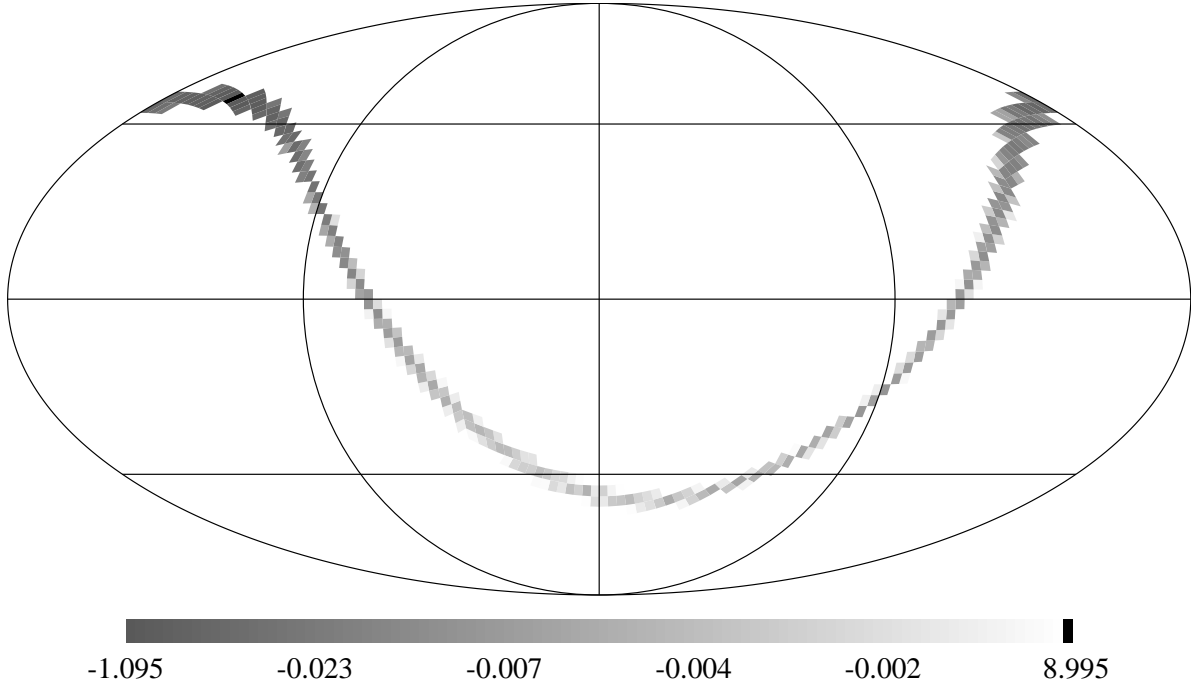


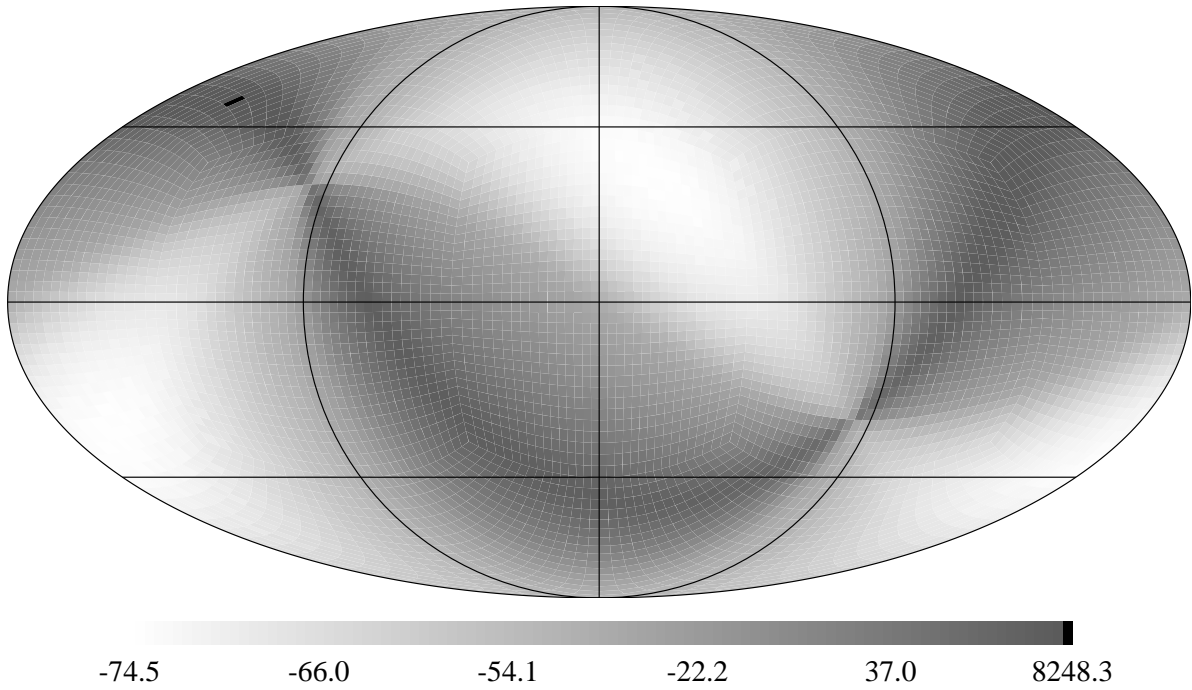| -88.6 | -79.6 | -60.8 | -18.5 | 35.5 | 6763.2 |

Fig. 5.— The row through the Lockman Hole of the correlation matrix **A** and the covariance matrix $\mathbf{A}^{-1}$ for the white noise case.

## Row of Correlation Matrix with 1/f Noise



| -1.095 | -0.023 | -0.007 | -0.004 | -0.002 | 8.995 |

## Row of Covariance Matrix with 1/f Noise



| -74.5 | -66.0 | -54.1 | -22.2 | 37.0 | 8248.3 |

Fig. 6.— The row through the Lockman Hole of the correlation matrix **A** and the covariance matrix **A**$^{-1}$ for the $1/f$ noise case. The $1/f$ knee is at $f_K = 10 f_{spin}$ so the effective chop angle is $13.4°$.
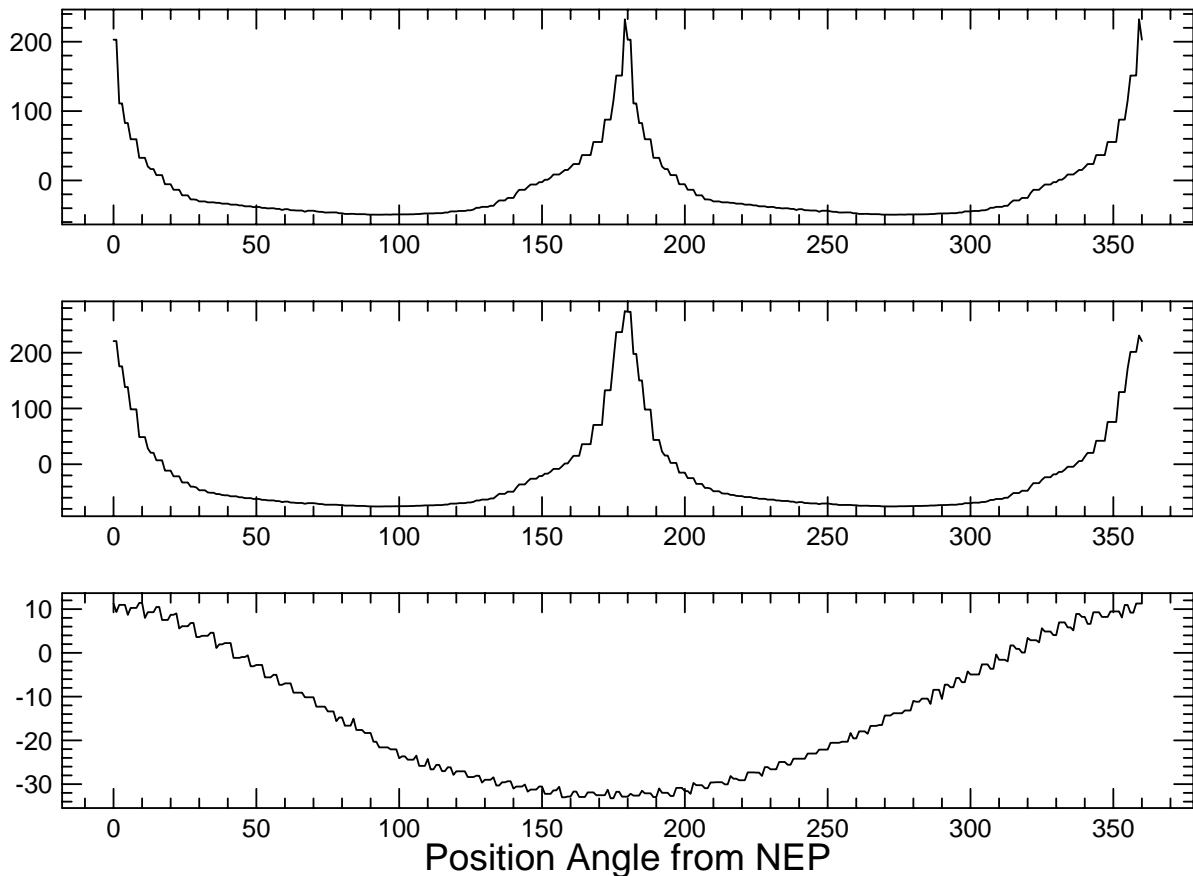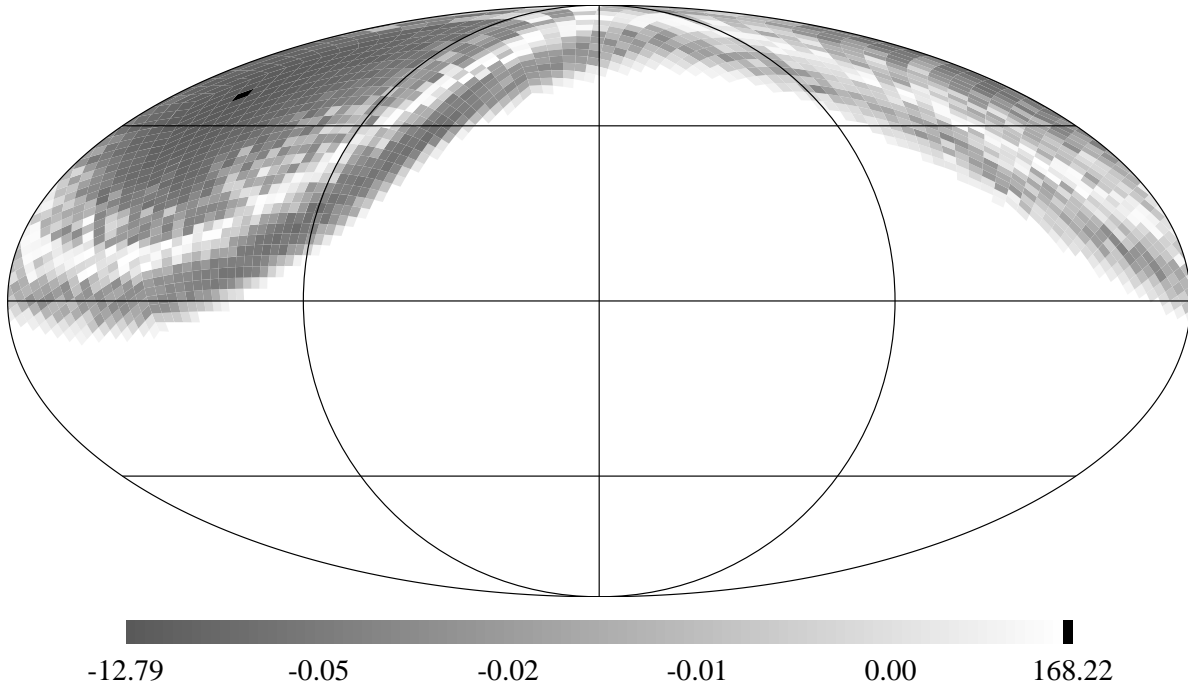
Fig. 7.— The covariance of pixels 90° from the Lockman Hole as a function of position angle with respect to the NEP for the white noise case (top) and the $1/f$ noise case (middle). Note the increased covariance on the scan circle through the Lockman hole at 0° and 180°. Bottom: the COBE scan case, with $1/f$ noise. Note the absence of stripes.

$b = 53°$. It was observed 10 times, which is close to the average exposure for the map. Figure 5 shows the white noise case. There is a small amount of excess noise and striping. The covariance matrices have been multiplied by the total number of data points, so a perfect experiment would have $n_p$ on the diagonal and $-1$ in the off-diagonal pixels. Figure 6 shows the $1/f$ noise case. There is a larger amount of excess noise and striping, but it is concentrated in the low order multipoles. The angle scanned during one radian at $f_K$ for this case is 5.7°, so excess noise in low multipoles is expected. Half of the weight in the baseline filter in Figure 2 is contained within $\pm 13.4°$ of the central pixel, so 13.4° is the effective chop angle. Figure 7 shows the covariance on a circle 90° away from the central pixel, which peaks sharply when crossing the scan circle – an indication of striping.

An even bigger example (Figure 8) shows the result of a one-horned experiment using the *COBE* DMR scan path with $1/f$ noise. One million data points were processed, and the orbit precession (yearly) rate was increased by a factor of 60 so these $10^6$ points covered a full annual cycle. The length of the pre-whitening filter was $L_W = 100$. Slow convolutions instead of FFT's were used to evaluate a row of $\mathbf{A}$ and to iterate to find a row of $\mathbf{A}^{-1}$. The time-ordered method

# Row of Correlation Matrix with COBE Scans



| -12.79 | -0.05 | -0.02 | -0.01 | 0.00 | 168.22 |

# Row of Covariance Matrix with COBE Scans



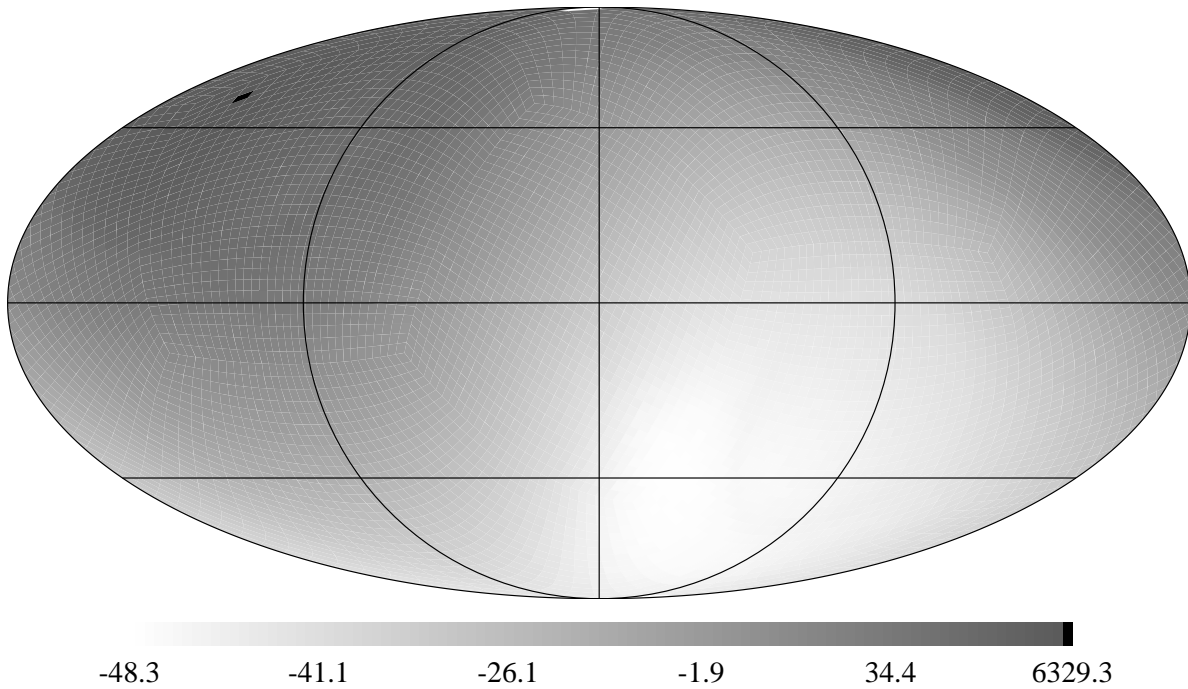| -48.3 | -41.1 | -26.1 | -1.9 | 34.4 | 6329.3 |

Fig. 8.— The row through the Lockman Hole of the correlation matrix $\mathbf{A}$ and the covariance matrix $\mathbf{A}^{-1}$ for the COBE scan case with $1/f$ noise. The $1/f$ knee is at $f_K = 5.5 f_{spin}$ so the effective chop angle is $11.8°$.

took 30 seconds on a workstation to evaluate a product of the form $\mathbf{AT}$. The residuals in $\mathbf{AT} = \mathbf{B}$ were reduced by a factor $10^{-5}$ after 20 iterations of the conjugate gradient method. These results are plotted at DMR resolution but the timing is independent of the number of pixels, $n_p$, and directly proportional to the number of data points, $n_d$.

The angle scanned in one radian at $f_K$ was $5.0°$, so the only advantage this case has over Figure 6 is that scans were made through each pixel in every direction. Thus it is not necessary to walk the baseline determination up to the NEP and then down along some other longitude. Thus the final covariance depends primarily on the distance between two points, giving a much more symmetric pattern in Figure 8. The Lockman Hole was observed 189 times, and the diagonal element of the covariance matrix is 0.00633, so there is 20% excess noise at the pixel level. The highest off-diagonal element in the Lockman Hole row is 8 times smaller than the diagonal element.

In general a symmetric covariance is much easier to analyze, since it leads to a noise level that depends only on $\ell$. But in the absence of systematic errors, Figures 5 and even 6 can give useful CMB data – especially if the overall noise level is low enough (Janssen *et al.* 1996).

## 7.    Systematic Errors

A systematic error term is a non-random signal in the time-ordered data that is not caused by the sky. Since true patterns on the sky form an $n_p$-dimension subspace in the $n_d$-dimensional data space, a systematic error term can be

1. Orthogonal to the sky subspace - these can be ignored.

2. Parallel to the sky subspace - these cannot be fixed.

3. At an intermediate angle to the sky subpsace - these must be measured and corrected.

Figure 9 shows these possibilities.

An example of a systematic error that is almost orthogonal to the sky subspace is the $B_y$ magnetic term in the *COBE* DMR. This is a susceptibility to a magnetic field along the axis perpendicular to the plane containing the plus and minus horns on a DMR. The bottom plot in Figure 10 shows the time-ordered data produced by this term, which can then be made into a map. That map is then converted back into time-ordered data, giving the top plot. Since the top and bottom plots are very different, it is easy to measure the $B_y$ sensitivity and correct for it.

A $B_z$ term is due to a sensitivity to magnetic fields in the plane defined by the horns but perpendicular to the spin axis. This produces a map with a large dipole aligned with the celestial pole. But the $B_z$ term is not completely parallel to the sky subspace because the Earth's magnetic dipole is offset and tilted so there is a diurnal modulation of the input shown on the bottom of Figure 11 that is not seen in the playback (top). Thus it is possible to measure a $B_z$ term and remove its effect from the map.

An example of a systematic error that is parallel to the sky subspace for a simple scan pattern perpendicular to the Sun-line through the ecliptic poles is zodiacal light emission. With the more
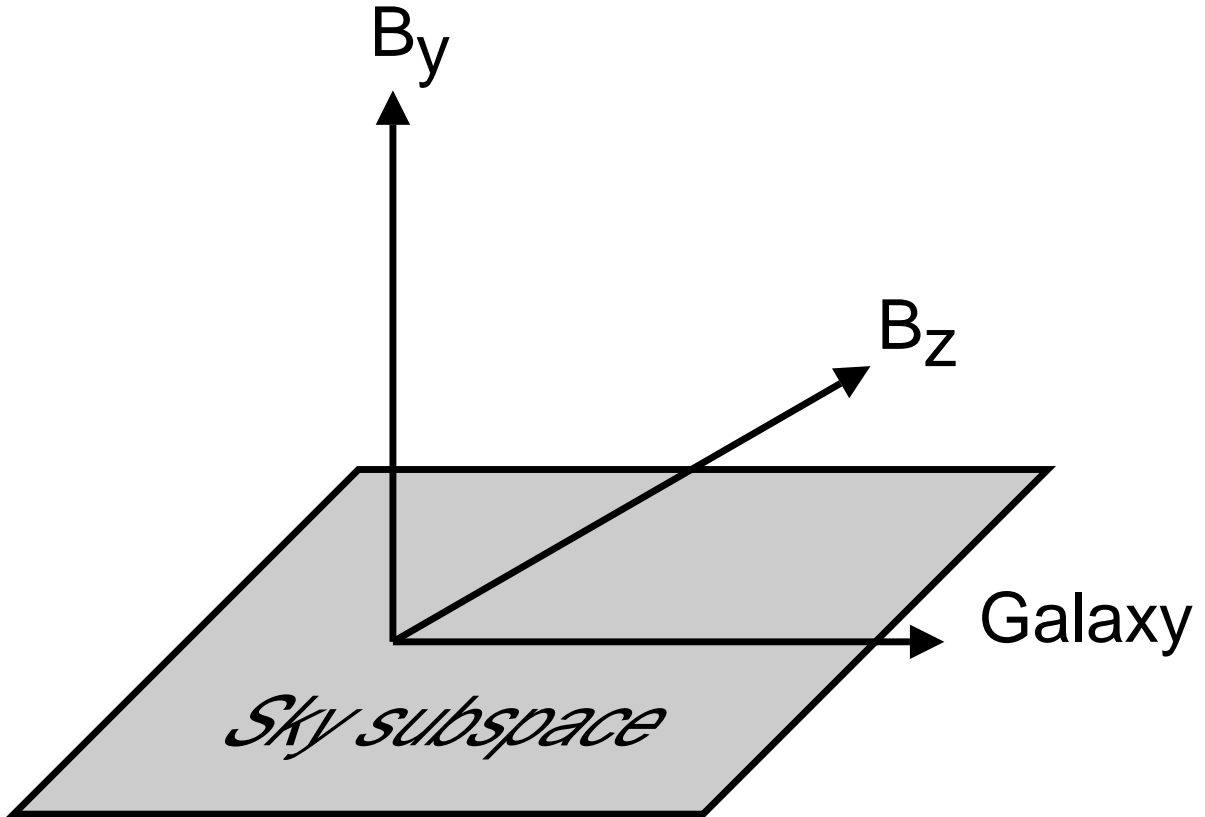
Fig. 9.— A diagram showing the $n_d$-dimensional "data space" and the $n_p$-dimensional subspace of sky patterns. A given systematic error is a direction in data space that can be also orthogonal to the sky subspace, like the $B_y$ magnetic effect, almost but not quite parallel to the sky subspace like the $B_z$ magnetic effect, or completely contained within the sky subspace like a galactic foreground (for 1 frequency maps).
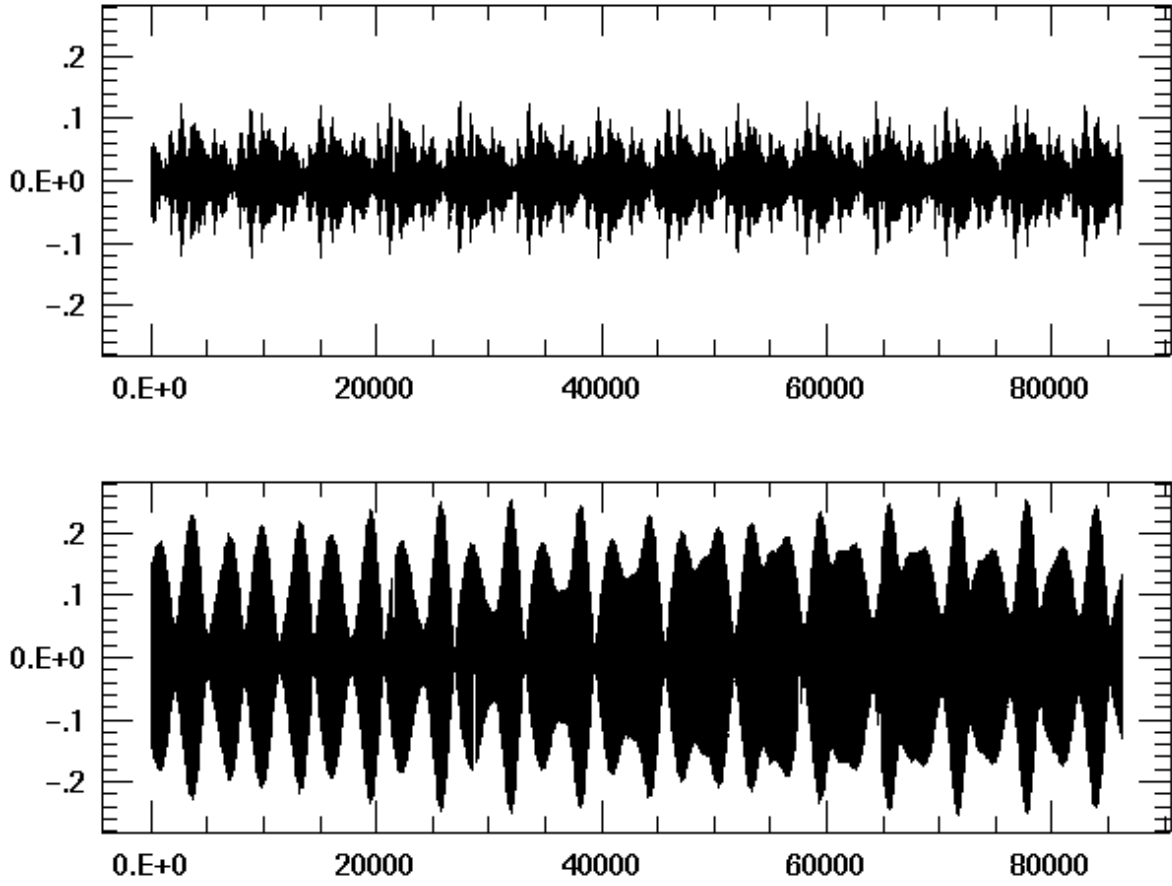
Fig. 10.— Bottom: Time-ordered signal in mK *vs.* seconds from a 1 mK/g *y*-axis magnetic sensitivity in the DMR. Top: Time-ordered signal resulting from a playback of the map created from the bottom input.
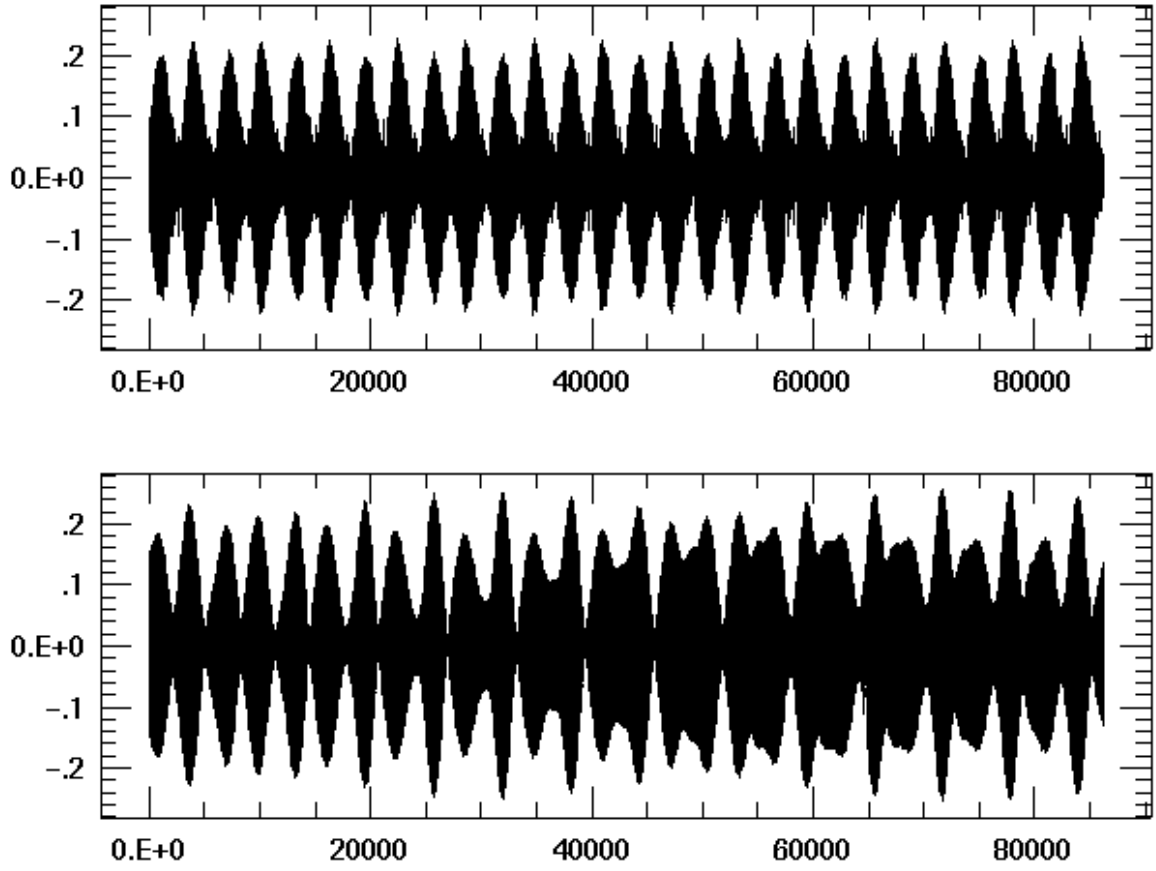
Fig. 11.— Bottom: Time-ordered signal from a 1 mK/g $z$-axis magnetic sensitivity in the DMR. Top: Time-ordered signal resulting from a playback of the map created from the bottom input.

complex scan pattern used by the DMR this effect can be measured and removed from the map.

## 8.    Desiderata

Obviously one should try to make all systematic errors orthogonal to the sky subspace. This is made easier if the data space is much larger than the sky subspace. Therefore the number of data points transmitted to the ground should be as large as possible, and on-board co-addition into scan circles should be avoided.

To avoid stripes, scans should be made through every pixel in all possible directions. This requires a large number of scans and a large number of data points, which are also desired to reduce systematic error problems.

## 9.    Conclusion

I have shown how to analyze large datasets from one-horned CMB experiments without simplified scan patterns that are vulnerable to systematic errors. The CPU time required is $\mathcal{O}(n_d \ln L_W)$ is differs from the Wright *et al.* (1996) differential method timing only in a logarithmic factor.

## REFERENCES

Bersanelli, M., Bouchet, F., Efstathiou, G., Griffin, M., Lamarre, J., Mandolesi, N., Norgaard-Nielsen, H., Pace, O., Polny, J., Puget, J., Tauber, J., Vittorio, N. & Volonte, S. 1996. Report on the COBRAS/SAMBA Phase A Study.

Janssen, M., Scott, D., White, M., Seiffert, M., Lawrence, C., Gorski, K., Dragovan, M., Gaier, T., Ganga, K., Gulkis, S., Lange, A., Levin, S., Lubin, P., Meinhold, P., Readhead, A., Richards, P. & Ruhl, J. 1996. astro-ph/9602007

Meyer, S. S., Cheng, E. S. & Page, L. A. 1991, ApJ, 371, L7

Wright, E. L., Hinshaw, G. & Bennett, C. 1996, ApJ, 458, L53-L56

---